Table 4.3.4.3. *Experimental and theoretical values for the coefficient α in the plasmon dispersion curve together with estimates of the cut-off wavevector (from Raether, 1980)*

	Measured α	Calculated α	q_c (Å^{-1})
Li	0.24	0.35	0.9
Na	0.24	0.32	0.8
K	0.14	0.29	0.8
Mg	0.35	0.39	1.0
Al	0.2 (<0.5 Å^{-1})		
	0.45 (>0.5 Å^{-1})	0.43	1.3
In	0.40 (<0.5 Å^{-1})		
	0.66 (>0.5 Å^{-1})		
Si	0.41		
	0.3	0.45	1.1

Table 4.3.4.4. *Comparison of measured and calculated values for the halfwidth $\Delta E_{1/2}(0)$ of the plasmon line (from Raether, 1980)*

	Experimental (eV)	Theory (eV)
Li	2.2	2.55
Na	0.3	0.12
K	0.25	0.15
Rb	0.6	0.64
Cs	1.2	0.96
Al	0.53	0.43
Mg	0.7	0.7
Si	3.2	5.4
Ge	3.1	3.9

in Fig. 4.3.4.3), is the *plasmon energy*, for which typical values in a selection of pure solid elements are gathered in Table 4.3.4.2. The accuracies of the measured values depend on several instrumental parameters. Moreover, they are sensitive to the specimen crystalline state and to its degree of purity. Consequently, there exist slight discrepancies between published values. Numbers listed in Table 4.3.4.2 must therefore be accepted with a 0.1 eV confidence. Some specific cases require comments: amorphous boron, when prepared by vacuum evaporation, is not a well defined specimen. Carbon exists in several allotropic varieties. The selection of the diamond type in the table is made for direct comparison with the other tetravalent specimens (Si, Ge, Sn). The results for lead (Pb) are still subject to confirmation. The volumic mass density is an important factor (through n) in governing the value of the plasmon energy. It varies with temperature and may be different in the crystal, in the amorphous, and in the liquid phases. In simple metals, the amorphous state is generally less dense than the crystalline one, so that its plasmon energy shifts to lower energies.

The above description applies only to very small scattering vectors **q**. In fact, the plasmon energy increases with scattering angle (and with momentum transfer $\hbar\mathbf{q}$). This dependence is known as the dispersion relation, in which two distinct behaviours can be described:

(*a*) For small momentum transfers ($q \lesssim q_c$), the dispersion curve is parabolic:

$$\hbar\omega_p(q) = \hbar\omega_p(0) + \frac{\alpha\hbar^2}{m_0} q^2. \qquad (4.3.4.9)$$

The coefficient α has been measured in a number of substances and calculated for the free-electron case in the random phase approximation (Lindhard, 1954); see Table 4.3.4.3 for some data. A simple expression for α is

$$\alpha = \tfrac{3}{5}\frac{E_F}{\hbar\omega_p(0)}, \qquad (4.3.4.10)$$

where E_F is the Fermi energy of the electron gas. More detailed observations indicated that it is not possible to describe the dispersion curve over a large momentum range with a single q^2 law. In fact, one has to fit the experiment data with different linear or quadratic slopes as a function of q [see values indicated for Al and In in Table 4.3.4.3, and Hohberger, Otto & Petri (1975)]. Moreover, anisotropy has been found along different **q** directions in monocrystals (Manzke, 1980). In parallel, refinements have been brought into the calculations by including band-structure effects to deal with the anisotropy of the dispersion relation and with the bending of the experimental curves. Electron–electron correlations have also been considered, which has slightly improved the agreement between calculated and measured values of α (Bross, 1978*a*, *b*).

(*b*) For large momentum transfers, there exists a critical wavevector q_c, which corresponds to a strong decay of the plasmon mode into single electron–hole pair excitations. This can be calculated using conservation rules in energy and momentum, giving

$$\hbar\omega_p(0) + \alpha\frac{\hbar^2}{m_0} q_c^2 = \frac{\hbar^2}{2m_0}(q_c^2 + 2q_c q_F), \qquad (4.3.4.11)$$

where q_F is the Fermi wavevector. A simple approximation is $q_c \simeq \omega_p/v_F$, v_F being the Fermi velocity. Single pair excitations can be created by fast incoming electrons in the domain of scattering conditions contained between the two curves:

$$\left.\begin{aligned} \Delta E_{\max} &= \frac{\hbar^2}{2m_0}(q^2 + 2qq_F) \\ \Delta E_{\min} &= \frac{\hbar^2}{2m_0}(q^2 - 2qq_F) \end{aligned}\right\} \qquad (4.3.4.12)$$

shown in Fig. 4.3.4.13. They bracket the curve $\Delta E = \hbar^2 q^2/2m_0$ corresponding to the transfer of energy and momentum to an isolated free electron. For momentum transfers such as $q > q_c$, the plasmon mode is heavily damped and it is difficult to distinguish its own specific behaviour from the electron–hole continuum. A few studies, *e.g.* Batson & Silcox (1983), indicate that the plasmon dispersion curve flattens as it enters the

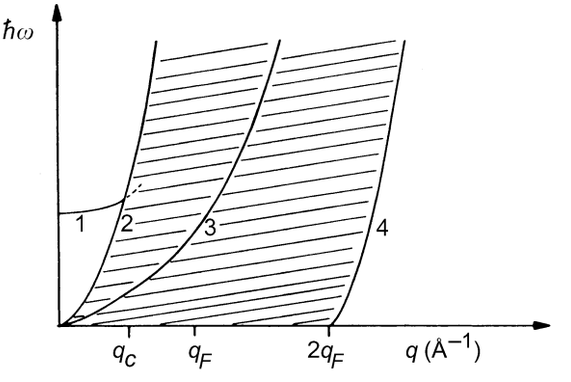

Fig. 4.3.4.13. The dispersion curve for the excitation of a plasmon (curve 1) merges into the continuum of individual electron–hole excitations (between curves 2 and 4) for a critical wavevector q_c. The intermediate curve (3) corresponds to Compton scattering on a free electron.

references